Quantifying the Effects of Atmospheric Stability on the Multifractal Spectrum of Turbulence

Bin Shi, Brani Vidakovic
School of Industrial and Systems Engineering
Georgia Institute of Technology, Atlanta, GA 30332-0205, USA
(e-mail:{bshi|brani}@isye.gatech.edu)

Gabriel G. Katul
Nicholas School of the Environment and Earth Sciences,Box 90328
Duke University, Durham, NC27708-0328, USA.
(e-mail:gaby@duke.edu)

March 30, 2004

Abstract

Over the past decade, several studies suggested possible analogy between price dynamics in the foreign exchange market and atmospheric turbulent flows. Such analogies suggest that applications in business and industry can directly benefit from detailed quantification of the scale-hierarchy existing in fully developed turbulent flows. Numerous studies have already demonstrated the multifractal properties of rough-wall boundary layer turbulence. How atmospheric stability (i.e. boundary conditions) alters the multifractal spectrum (MFS) of turbulent velocity and temperature fluctuations in the atmospheric surface layer remains to be investigated. A challenge of estimating the MFS from time series via traditional regression approaches is the heteroskedastic problem because the variance of the error term are shown to depend on scale. Using a combination of Discrete Wavelet Transforms (DWT) and a Weighted Least Squares (WLS) scheme, heteroskedastic effects are minimized and robust estimation of the scaling parameters needed to compute the MFS is derived. Next, to quantify the effects of atmospheric stability on the MFS, discriminative measures that utilize the left slope (rise), Hurst exponent (maxima), and broadness are employed. Distributional property of the estimators for

these discriminative measures are investigated based on Monte Carlo simulations. These summary measures are applied to the MFS of velocity and temperature time series collected in the atmospheric surface layer for a wide range of atmospheric stability conditions. The criteria for success in evaluating how atmospheric stability alters the MFS of a single flow variable time series is formulated as a statistical classification model that properly infers the stability regime when these three discriminative measures are used as input vectors.

Keywords: Wavelet, Multifractal Spectrum, Weighted Least Squares, Turbulence, k-NN Classification.

1 Introduction

It is now recognized that many processes in nature, engineering, science, and economics exhibit complex scaling behavior. This complexity in scaling is commonly reflected by an inhomogeneity in the irregularity of fluctuating patterns, i.e., an irregularity that can switch from one pattern to another at any time. The availability of high-frequency data for financial markets has made it possible to study market dynamics on timescales of less than a day. For foreign exchange, there is a net flow of information from long to short timescales: the behaviour of long-term traders (who watch the markets only from time to time) influences the behaviour of short-term traders (who watch the markets continuously). Motivated by this hierarchical feature, several studies have already reported striking analogies between these dynamics and atmospheric turbulence [10]. Hence, multiscale methodologies developed to analyze the hierarchical structure of turbulence can provide an organizing framework for analyzing such flow of information.

Theoretical arguments based on the Navier-Stokes equations and statistical analysis of numerous experiments have shown that turbulence is representative of complex processes rich in variability across broad range of time scales. "Multifractal analysis" was originally suggested by [9] to analyze such complex phenomena in turbulence. The Multifractal analysis assumes that local singularities exist within the process and are organized in nested fractal sets (for a rigorous mathematical theory of multifractal processes see [22, 21]). In turbulence, this assumption deviates from the classical Kolmogorov $K41$ law in which the turbulence is assumed to posses a constant scaling behavior characterized by a single Hurst exponent of $1/3$ ([17]). The anomalous scaling (i.e. multifractality) of turbulence is commonly attributed to short-circuiting of the energy cascade due to the existence of

organized large-scale features such as ramp-like structures, which are influenced by boundary conditions, and themselves directly influence small scale turbulence [25, 6]. A logical question to explore is whether measures of multifractality, such as the multifractal spectrum (MFS), are affected by boundary conditions such as surface heating and friction velocity or a combination thereof such as atmospheric stability. The MFS describes the "richness" of the process in terms of local strengths of singularities. The term spectrum denotes the spectral decomposition of the process into components characterized by their irregularity. Roughly speaking, the MFS could be regarded as the probability distribution of the local strength of singularities.

In this paper, we seek to address the following problem: how does atmospheric stability alter the MFS of atmospheric surface layer (ASL) turbulence. Towards this end, we use longitudinal (u), lateral (v), and vertical (w) velocity along with virtual potential temperature (T) time series measurements collected in the ASL for a wide range of stability conditions of a grass-covered surface.

There are two obstacles to addressing this problem: The first deals with the estimation of the MFS from limited time series, and the second deals with assessing how atmospheric stability alters key attributes describing the MFS. The estimation of the MFS relies on the multifractal formalism which has been developed using different mathematical tools. In recent years, the multifractal formalism and the estimation of MFS via discrete wavelet transforms (DWT) received popularity ([3]). The advantage of using a wavelet-based multifractal spectrum is (i) the availability of the fast algorithms, (ii) automatic separation of trends and fluctuations, and (iii) the widely demonstrated effectiveness in various applications ([3],[24]). We show via DWT that a weighted-least squares method that reduces the inherent heteroskedasticity in estimating local scaling parameters is also possible.

One approach to address how atmospheric stability alters the MFS is to quantify whether large changes in atmospheric stability produce measurable departure in scaling parameters of a standard cascade model fitted to the data (such as β and random β models). In this paper, we go beyond and use a more general approach that does not depend on the specifics of the cascade model but directly analyzes the effects of atmospheric stability on geometric attributes of the MFS.

The remainder of the paper is organized as follows: Section 2 briefly describes the dataset used. Introductory overview of wavelet-based multifractal spectrum is given in Section 3. Quantitative characteristics of the multifractal spectrum are discussed in Section 4. Next, the proposed spectral features are estimated and applied to the problem of identifying the

stability condition of the turbulence flow measurements, as will be provided in Section 5. The conclusions and recommendations are presented in Section 6

2 Data

Time series measurements of u,v w, and T were collected over a grass-covered forest clearing at Duke Forest near Durham, North Carolina. The measurements were collected on June, 12-16, 1995 at 5.2 m above the grass surface using a GILL triaxial sonic anemometer. Sonic anemometers measure velocity by sensing the effect of wind on transit times of sound pulses traveling in opposite directions across a known instrument distance $d_{sl} =$ (0.149 m in this study). The measurements were sampled at $f_s = 56Hz$ and were subsequently divided into 19.5 minute intervals to produce $N = 65,536$ time measurement per flow variable per run. Our choice of 19.5 minute intervals is a compromise between the need for stationary conditions at large scales and maximizing the statistical sample size within a given run. We focus on an ensemble of 95 runs (6 of them are from the stable regime, 23 are neutral and the rest are unstable) collected over a wide range of stability conditions ranging from near convective to stable atmospheric flows. The ensemble size of all combined runs per flow variable exceeds 6.75×10^6 time measurement (but the analysis is conducted on individual runs prior to ensemble averaging). Further details about the experimental setup, atmospheric stability conditions, inertial subrange identification, and instrumentation details can be found elsewhere [15, 16].

To exploit the usage of the available data and overcome the difficulty of collecting stable and neutral measurements, each time series is segmented into pieces, each with a length of 4096.

3 Wavelet-based Multifractal Spectrum

Given that our analysis is based on the multifractal spectrum formalism, a brief review is provided below. The wavelet-based calculation of a multifractal spectrum depends on the concepts of *partition function* and *Legendre transform*. The partition function $T(q)$ is defined as

$$T(q) = \lim_{j \to -\infty} \log_2 E|d_{j,k}|^q, \tag{1}$$

where $d_{j,k}$ is the $\mathcal{L}_1$-normalized wavelet coefficient at level j and position index k, and q is the order of moments. We emphasize that q is real and can

be positive or negative. However, the interpretation of negative moments is still not clear (or physical). This partition function incorporates various orders of moment information that are believed to be fundamental in multifractal analysis. In fact, change in $T(q)$ with respect to q correspond to inconsistent Hurst estimators (corresponding to different values of q) $H(q)$ if monofractality is assumed.

Even though (1) is informative, the singularity measure is not explicit. It has been proposed in [11] that the local singularity strength can be measured in terms wavelet coefficients as :

$$\alpha(t) = \lim_{k2^j \to t} \frac{1}{j} \log_2 |d_{j,k}| \tag{2}$$

It has been shown [14] that the wavelet coefficients preserve the scaling behavior of the process if the wavelet is more regular than the process. The local singularity strength measures (2) converges to the local Holder index of the process at time t. Here, $\alpha(t)$ measures the oscillation of the process at time t. Small values of $\alpha(t)$ reflect more irregular behavior at time t. Any inhomogeneous process has a collection of local singularity strength measures and their distribution $f(\alpha)$ which forms the multifractal spectrum. A direct way to obtain this spectrum is to use the counting technique,

$$f(\alpha) = \lim_{\epsilon \to 0} \#\{\alpha(t) : \alpha - \epsilon < \alpha(t) < \alpha + \epsilon, -\infty < t < \infty\}. \tag{3}$$

Although it is feasible to estimate the multifratcal spectrum using (2) and (3), the method is not practicable due to the difficulty of approximating the limit and the computational expense. A useful tool to improve the estimation efficiency is the Legendre transform. The Legendre transform of the partition function is

$$f_L(\alpha) = \inf_q \{q\alpha - T(q)\}. \tag{4}$$

It can be shown that $f_L(\alpha)$ converges to the true multifractal spectrum using the theory of large deviations [8].

From the practical point of view, we still require a robust estimator of the partition function. If we rearrange (1), it becomes,

$$E|d_{j,k}|^q \sim 2^{jT(q)}, \quad \text{as} \quad j \to -\infty \tag{5}$$

On the other hand, it has been shown that the qth moment of the wavelet coefficients of the power law process [3] satisfies the following equation:

$$E|d_{j,k}|^q = C_q 2^{jqH} \tag{6}$$

where H is the so-called self-similarity exponent and C_q is a constant depending only on q. Comparing (5) and (6), one can relate the partition function estimation with the self-similarity exponent estimation problem. It is a standard practice to use linear regression to identify the self-similarity exponent H since the values $E|d_{j,k}|^q$ could be easily obtained by moment-matching method thereby facilitating the estimation of $T(q)$. Formally speaking,

$$\log_2 \widehat{S_j(q)} \sim jT(q) + \varepsilon_j, \tag{7}$$

where $\widehat{S_j(q)} = \frac{1}{N2^{-j}} \sum_{k=1}^{N2^{-j}} |d_{j,k}|^q$ is the empirical q^{th} moment of the wavelet coefficients (N is the length of the entire time series) and the error term ε_j is introduced from the moment matching method when replacing the true moments with the empirical ones. Simple ordinary least square (OLS) is the most convenient choice of estimating the partition function. However, the bias can be very large in some extreme cases since the variance of the empirical q^{th} moments is not constant with respect to scale j. The variance of $\log_2 \widehat{S_j(q)}$ is

$$Var(\log_2 \widehat{S_j(q)}) = \frac{A(q)}{N2^{-j}} + \frac{B(q)}{N^2 4^{-j}} + \cdots \tag{8}$$

where $A(q)$ and $B(q)$ are constants depending only on the underlying distribution function of the finest wavelet coefficient. Therefore, it is clear that the regression problem in (7) is a heteroskedastic problem in which the variances of the error terms are not constant across the scales. Even though the OLS solution of $T(q)$ is still unbiased and consistent asymptotically, it is no longer efficient due to the heteroskedasticity. To resolve this problem, weighted least squares (WLS) is used to obtain efficient unbiased estimates. WLS estimator downweights the squared residuals for scales with large variances, in proportion to those variances. If one finds $w_j = Var^{-1}(\log_2 \widehat{S_j(q)})$, a WLS estimator of $T(q)$ is given by

$$\widehat{T(q)} = \frac{\sum_{j=1}^{J} w_j \sum_{j=1}^{J} j w_j \log_2 \widehat{S_j(q)} - \sum_{j=1}^{J} j w_j \sum_{j=1}^{J} w_j \log_2 \widehat{S_j(q)}}{\sum_{j=1}^{J} w_j \sum_{j=1}^{J} j^2 w_j - (\sum_{j=1}^{J} j w_j)^2} \tag{9}$$

In practice, the exact analytical formula $Var(\log_2 \widehat{S_j(q)})$ is too complicated to be used directly. However, if the N is reasonably large (as is the case here), the first term in (8) will be dominant. Therefore, it is natural to use the approximate weights $p_j = N2^{-j}$. This WLS estimator results in a variance given by,

$$Var(\widehat{T(q)}) = \frac{A(q)C(J)}{N} + \frac{B(q)D(J)}{N^2} \tag{10}$$

where the constants $C(J)$ and $D(J)$ can be evaluated from the formula provided in [4].

Once the $T(q)$ is estimated, the next step is to perform the Legendre transform. Since $\frac{\partial(\alpha q - T(q))}{\partial q} = \alpha - T'(q)$ and $T''(q) < 0$ ([11]), the maximum value of $\alpha q - T(q)$ is achieved at $q = T'^{(-1)}(\alpha)$. So, performing the Legendre transform is divided into two steps: First, the numerical derivative of $T(q)$ is obtained using the finite difference; then, the value of Legendre spectrum at $\alpha = \widehat{T'(q)}$ is evaluated. We point out that the Legendre transform is not able to estimate the multifractal spectrum value at arbitrary singularity strength α. The set of the multifractal spectrum values is determined by a pre-specified vector of q values. The more q values used, the finer the multifractal spectrum will appear, i.e., the resolution of the spectrum is determined by the "(order) sampling frequency" of the moments.

4 Geometric Attributes of the Multifractal Spectrum

Theoretically, the multifractal spectrum of a fractional Brownian Motion or fBm process (representative of mono-fractals) consists of three geometric parts: the vertical line (slope=$+\infty$), the maximum point and the right slope (slope=1) [11]. The maximum point corresponds to the Hurst exponent and the vertical line and the right slope are thought to be inherent features, which distinguish fBm from a multifractal process. However, it is rare to obtain such a perfect spectrum in practice. Even for a well simulated fBm, due to finite sample size and estimation error (the partition function estimation and derivative approximation are responsible for most of the errors), its spectrum may deviate from the theoretical form, as shown in Figure 1. Even with the lack of precise estimation of the spectrum, the extent of deviation from the vertical line could be still utilized in the discrimination between the mono- and multi-fractal processes. In Figure 1, two processes are presented. One is the fBm and the other is the turbulence measurement (horizontal velocity randomly taken from the dataset described in Section 2), which is widely believed to be a multifractal process. Comparing with the turbulence measurement, the fBm is much closer to the vertical line and this closeness may be quantified by the left slope of the spectra. Another important difference between these two spectra is the width spread of the spectra. It is obvious that the width spread of the fBm is much smaller than that of the turbulence measurement indicating lack of richness in singularity indices for the fBm.

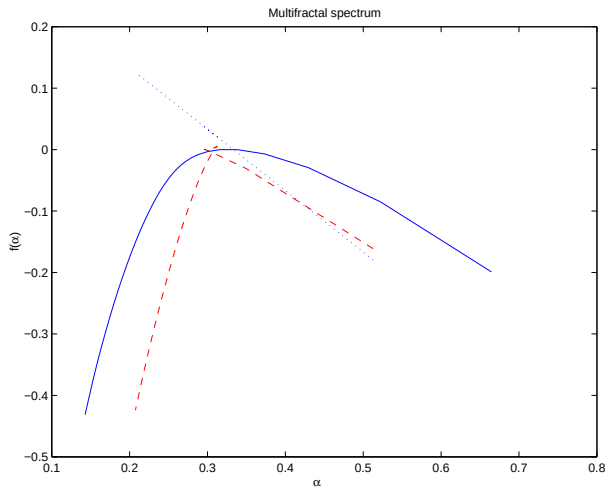

Figure 1: Multifractal Spectra for mono- (dash line) and multifractal (solid line) processes. The dotted line indicates the theoretical slope of the spectrum for a monofractal process)

Despite the estimation error, the spectrum can be approximately described by two slopes and one point without loss of the discriminant information. Alternatively, we can also approximate the key "geometric" features in the spectrum by the left slope, the maximum point, and the width spread. A typical multifractal spectrum can be quantitatively described as shown in Figure 2. Here, we choose the left slope, the maximum point and the width spread to discriminate the multifractality. This is verified by an empirical study (described later).

The left and right slopes can be obtained using linear regression. However, it is not straightforward to compute the width spread automatically. This difficulty can be attributed to - (i) automatically locating the start and end points of the width spread, and (ii) the discreteness of the spectrum. The former is difficult conceptually while the latter is difficult computationally. There are many ways to define the width spread. In this paper, we select the definition with the most practical success and name it the *broadness* of the spectrum, discussed next.

Definition: Suppose that α_1 and α_2 are two roots that satisfy the equation $f(\alpha) + 0.2 = 0$ and $\alpha_1 < \alpha_2$. The broadness of multifractal spectrum is defined as $B = \alpha_2 - \alpha_1$, where $f(\alpha)$ is the spectrum function in terms of Holder regularity indices α's.

This definition is also graphically presented in Figure 2. The deviation from the mono-fractal could be computed according to this Broadness measure since it posts a universal standard on the width spread. It is worth to point out the threshold value 0.2 used in this definition could be adjusted empirically to insure that this measure is well defined for all analyzed signals. As mentioned in the previous section, the choice of threshold value is correlated to the choice of q and the inherent data characteristics because these are the factors that affect the resolution of the spectrum. The discreteness may also produce difficulties in the computation. The problem is that it may be difficult to obtain exact roots of the equation $f(\alpha) + 0.2 = 0$ from the set of discrete values of α. To bypass this issue, we compute the minimum value of $|f(\alpha) + 0.2|$ with respect of α instead of directly solving the equation.

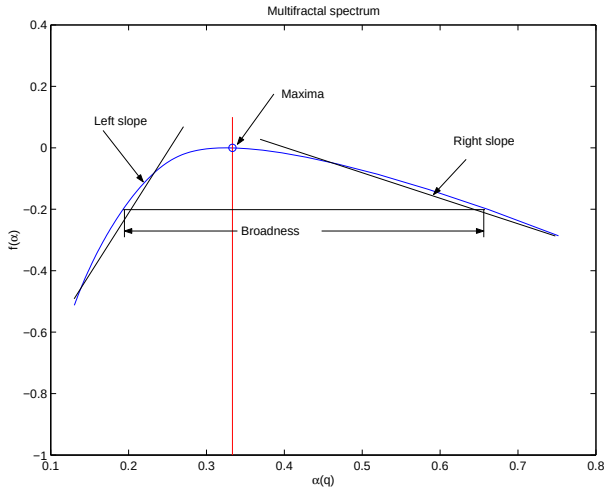

Figure 2: Canonical features of the MFS, including the Broadness measure.

Another problem we want to address is the distribution property of the geometric attribute estimators. Since the estimation of MFS involves Legendre transform, which is not a regular function, it becomes a nontrivial problem to derive the asymptotic distributions of MFS. However, Monte Carlo simulation lends power to gain some insights of these distributions. Figure 3 shows these simulation results. We generate 1000 sample paths of fBm each with Hurst parameter 1/3 and length 4096. Then, we estimate MFS and its geometric attributes for each path. Next, the collections of geometric attributes are plotted as normal quantiles to check the normality of these attribute estimators. The linearity of the QQ-plot appeared in the

middle plot of Figure 3 suggests that our estimate of Hurst based on MFS maxima is asymptotic normal. The descriptive statistics also show that it is an unbiased and consistent estimator. However, the left and right QQ-plots in Figure 3 indicate that the corresponding estimators are not normal because of the significant curvature at the tails of these plots. So, even under the assumption that process is Gaussian, the normality conclusions about all estimators are not universal.

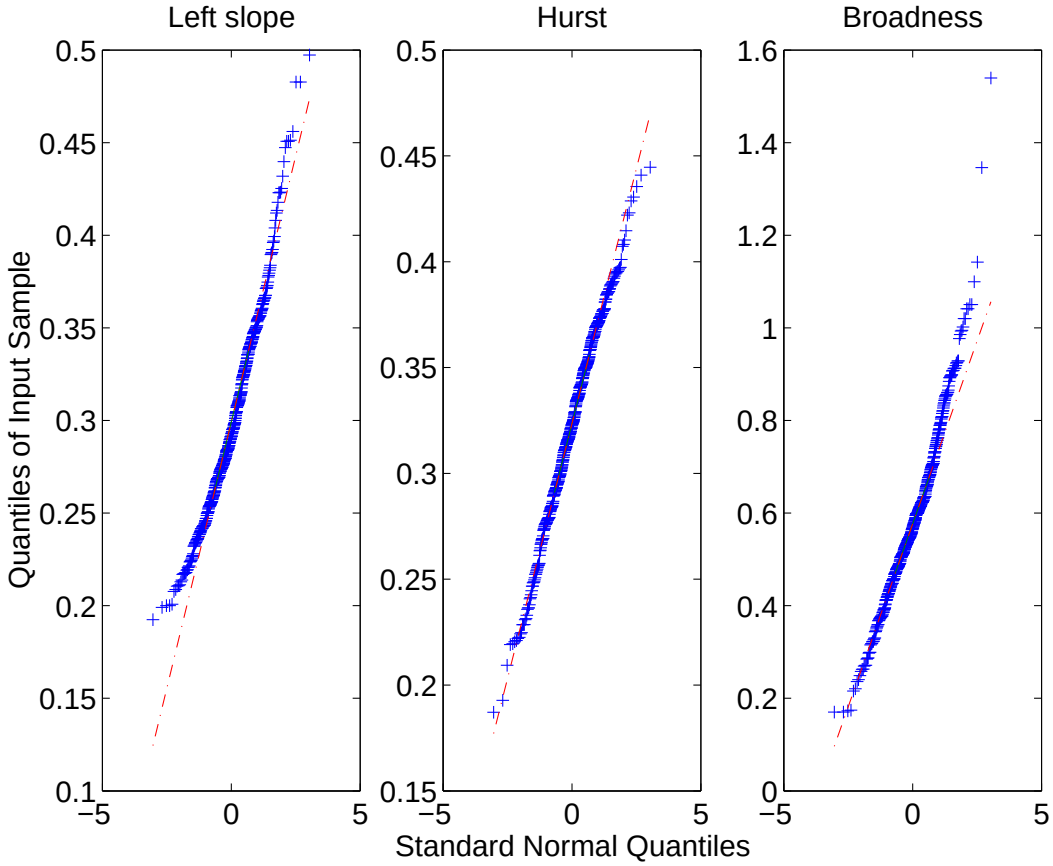

Figure 3: QQ plots for Left slope, Hurst exponent, and Broadness based on 1000 Monte Carlo replicates of fBm sample paths

5 The Effects of Atmospheric Stability Conditions on the MFS

In this section, we discuss how the geometric attributes of MFS of all four flow variables are influenced by atmospheric stability. We computed the broadness, Hurst exponent, and left slope for each measurement run and flow variable collected for the three different atmospheric stability regimes. Table 1-4 summarize the MFS characteristics of the four turbulent flow variables u, v, w and T. It is clear from these tables that among the three MFS geometric attributes, broadness varies most with atmospheric stability class, and hence will be used as the key variable in the analysis below.

Table 1: Summary statistics of the multifractal spectra for the horizontal velocity u

Stability		Left slope	Hurst	Broadness
Stable	Mean	0.3411	0.3755	0.6308
	Std.	0.0692	0.0607	0.2052
Neutral	Mean	0.3482	0.4093	0.6198
	Std.	0.0672	0.0668	0.1825
Unstable	Mean	0.3397	0.4071	0.6306
	Std.	0.0528	0.0623	0.18

Table 2: Summary statistics of the multifractal spectra for the lateral velocity v

Stability		Left slope	Hurst	Broadness
Stable	Mean	0.3568	0.3592	0.564
	Std.	0.1133	0.0948	0.2019
Neutral	Mean	0.3371	0.3963	0.5941
	Std.	0.046	0.0527	0.1514
Unstable	Mean	0.343	0.3987	0.6322
	Std.	0.0541	0.0676	0.1872

To visualize the discriminative information embedded in these spectral characteristics, a bivariate kernel based density of the broadness and Hurst exponents are estimated and contours of these densities are presented in Figure 4-5 with centroid points indicated as '+'. By observing these distributions, we conclude that the correlations between broadness and Hurst measures are insignificant since these contours are symmetric with both hor-

Table 3: Summary statistics of the multifractal spectra for vertical velocity w

Stability		Left slope	Hurst	Broadness
Stable	Mean	0.3427	0.3694	0.6115
	Std.	0.0442	0.0743	0.1673
Neutral	Mean	0.3541	0.3779	0.5892
	Std.	0.0454	0.0623	0.1434
Unstable	Mean	0.349	0.3922	0.6526
	Std.	0.0569	0.0731	0.183

Table 4: Summary statistics of the multifractal spectra for air temperature T

Stability		Left slope	Hurst	Broadness
Stable	Mean	0.3399	0.3308	0.589
	Std.	0.0733	0.1113	0.1839
Neutral	Mean	0.3205	0.2796	0.6133
	Std.	0.0665	0.0658	0.2407
Unstable	Mean	0.371	0.4135	0.6234
	Std.	0.0806	0.1386	0.2033

izontal and vertical axis. This symmetry implies that their marginal distributions are orthogonal to each other. The variability of the measures among a certain stability regime is measured by the contour area. In these plots, the close curves correspond to the 20%, 50% and 80% confidence regions respectively from the inside to outside. The layout of these three closed curves also indicate the symmetry, flatness, and heavy tails of the distributions. For the velocity variables u, v w, the distributions from the unstable regime are more symmetric than those from the other two regimes. Even though the locations of distributions for the four velocity do not depend much on stability conditions, there is a large difference for the temperature variable T. The distribution under neutral stability shifts to the left very much. It is clear that the bivariate kernel distributions of Hurst and broadness are quite sensitive to the stability regimes, especially between unstable and stable and for all 4 flow variables. This analysis does demonstrate that atmospheric stability can dramatically impact the MFS of all the variables.

Besides the joint distributions of Hurst and Broadness, we also estimate those of other two pairs: (1) Hurst and Left slope (2) Left slope and Broadness. The contour plots of these distribution (not shown)suggest that among these three pairs, Hurst and Broadness produce the most discriminative distributions for all of the four flow variables.

A rigorous test regarding the sensitivity of the MFS to the stability class can be formulated as follows: Given the MFS of a flow variable, as derived from a time series, can we distinguish between the three stability classes (neutral, unstable, and stable).

The crucial part of this test is to build a class boundary in terms of the MFS spectral characteristics for the measurements with different stability conditions. This coincides with the statistical classification problem. Simply looking at the contour plots of bivariate distributions in Figure 4-5, we expect the linear boundary may not be appropriate. The nonlinearity of the boundary must be taken into consideration. In this study, MFS spectral characteristics are selected as input vector and their distributions are not Gaussian as found in section 4. The deviation from normality for the input vector and the nonlinearity of the boundary motivates choosing k-nearest-neighbor (k-NN) classifier as the model. The data-adaptive property of k-NN makes it able to produce the nonlinear boundary. Also, k-NN is a very flexible classifier in the sense that it requires minimum assumption on the distribution of the input vector. For more details about the k-NN classification, see [12]. The steps of our testing is the following: First, we divide the original data set into two parts following the standard 2-fold scheme, i.e., for each stability condition, 80% of the measurements go to

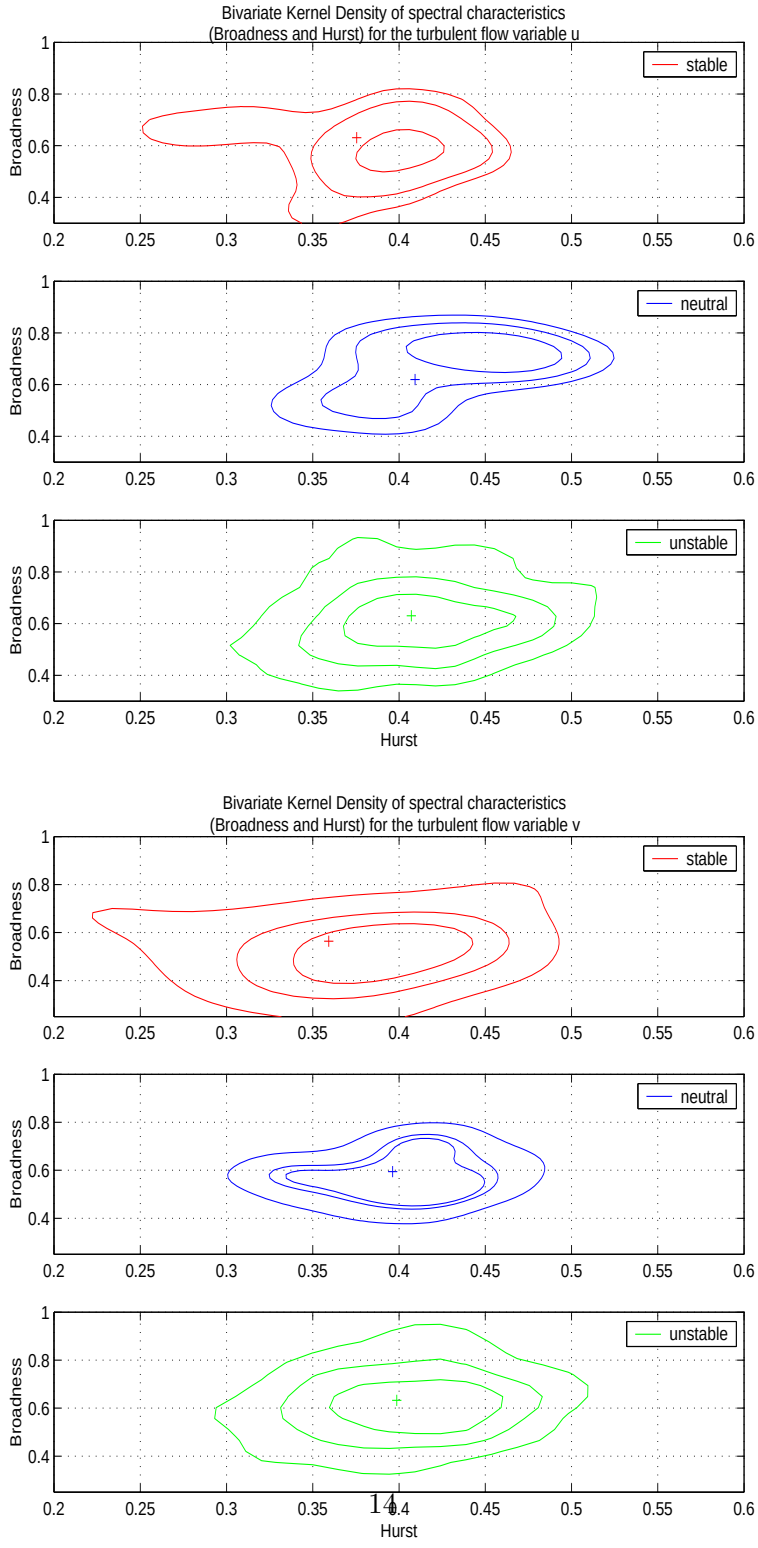

Figure 4: Joint probability density of the Hurst exponent and Broadness for flow variable u and v

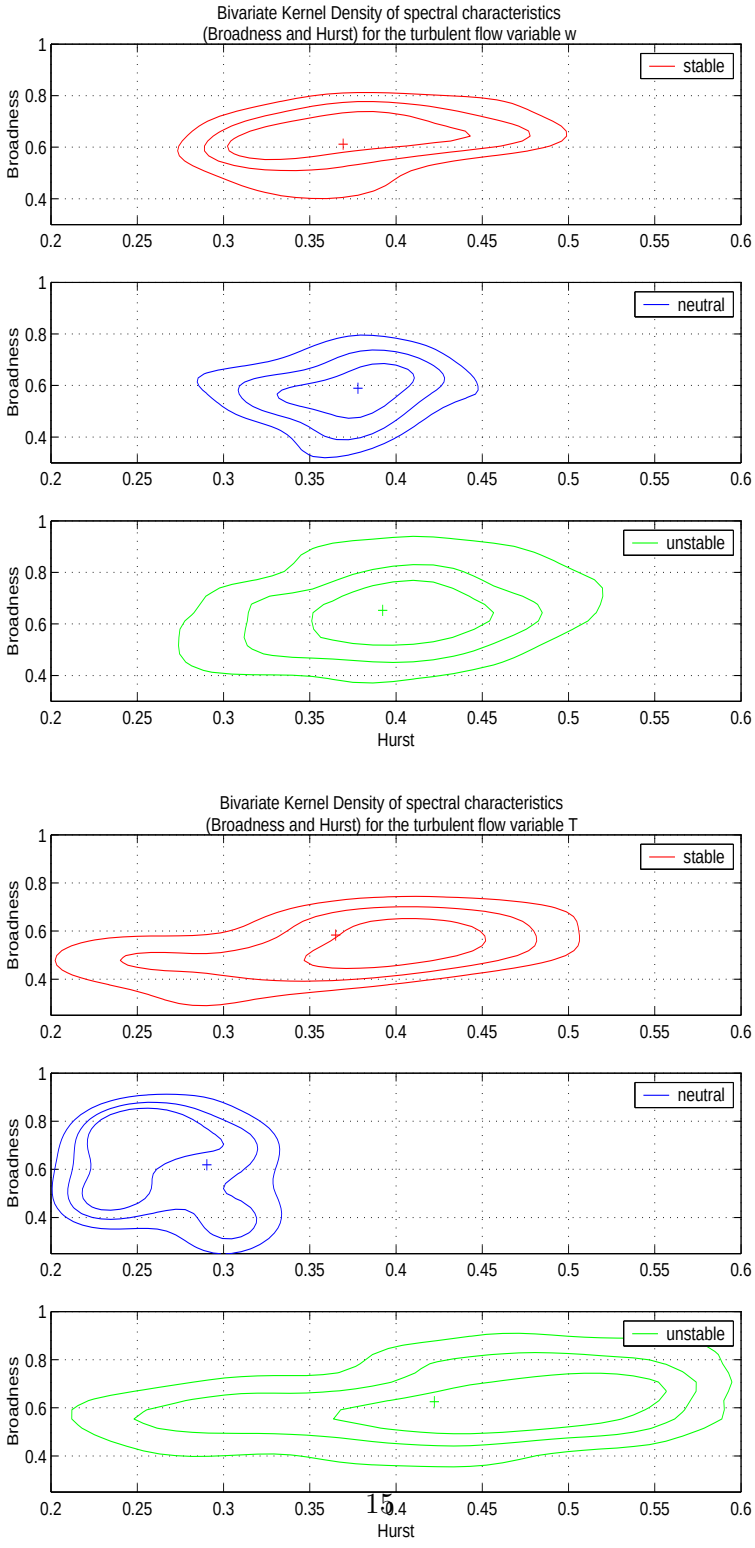

Figure 5: Joint probability density of the Hurst exponent and Broadness for flow variable w and T

the training set, which is used to estimate the parameters of the model, the other 20% measurements are used to verify the predicative accuracy of model and hence called test set. Next, the MFS spectral characteristics are calculated for each measurement. These characteristics form the feature space. Then, the Euclidian distance in the feature space is used to determine k elements in training set closest to the unknown sample. The class of the unknown sample is then defined by the mode of the classes distribution of the k elements. The k-NN classification results are reported in Table 5. The error rate here could be regarded as the empirical probability of committing a mistake if we assume that the multifractal spectral characteristics of the measurements are really sensitive to the stability class. From Table 5, all of the error rates are relatively small. So, we have more than 90% confidence to guess the stability class from the MFS. Among these four variables, v is the least likely to be misclassified while w is most likely.

Table 5: Stability condition classification prediction of the turbulence measurements using k-nearest-neighbor classifiers

	velocity u	velocity v	velocity w	temperature T
Training error	0.079	0.0749	0.0869	0.0814
Test error	0.0841	0.0773	0.0844	0.0822

6 Conclusions

This study is among the first to address the problem of quantifying the effects of atmospheric stability on the multifractal spectrum of turbulent flow variables u, v, w and T. We developed a wavelet-based estimator of the multifractal spectrum and proposed to use WLS in the regression step to improve the robustness of the estimation. We showed that the latter method is able to overcome the difficulty of dealing with the heteroskedastic effects caused by the scale-dependent moment estimators. A suitable weight function in practical problems is also derived. To efficiently compare the spectral characteristics for different variables and stability conditions, we defined the geometric attributes of the multifractal spectrum (GAMFS). The GAMFS of turbulent flows u, v, w and T within different stability are then estimated and empirically compared using descriptive statistics and kernel bivariate densities. We found that stability conditions do have different impacts on u, v, w and T. Overall, the GAMFS of neutral measurements are quite different from those of the other two types of measurements. A

rigorous test regarding the sensitivity of the MFS to the stability class was formulated as a statistical classification problem. The universally small test errors suggest significant sensitivity of GAMFS to the four flow variables and to the stability conditions.

The broader impact of this work is a robust methodology that can detect shifts in the multiscale properties of stochastic processes (e.g. MFS). We showed that GAMFS were able to detect shifts in MFS when ASL turbulence experienced shifts in stability regimes. Hence, it is likely that GAMFS can also shed some light on the debate about the similarity between ASL turbulence and the price dynamics in the foreign exchange market (e.g. [19]).

Acknowledgement

Work of Shi and Vidakovic was supported by National Science Foundation (NSF-DMS-0072585) at Georgia Institute of Technology. Katul acknowledges support from the National Science Foundation (NSF-DMS-0072585 and NSF-EAR-0208258) at Duke University. The field experiment was supported by the Biological and Environmental Research (BER) Program, United States Department of Energy, through the Southeast Regional Center (SERC) of the National Institute for Global Environmental Change (NIGEC), and through the Terrestrial Carbon Processes Program (TCP).

References

[1] Abry, P, Gonçalvès, P, and Flandrin, P. Wavelets, Spectrum estimation, 1/f processes. *Wavelets and Statistics, vol. 105 of Lecture Notes in Statistics* , Springer-Verlag, New York, 1995; 15-30.

[2] Abry, P, and Veitch, D. Wavlet analysis of long rang depedent traffic. *IEEE Trsanctions on Information Theory.* 1998; **44**, 2-15.

[3] Arneodo, A, Bacry, E, Jaffard, S, and Muzy JF. Singularity spectrum of multifractal functions involving oscillating singularities. *Journal of fourier analysis and applications.* 1998; **4**, 159-174.

[4] Audit, B, Bacry, E, Muzy, JF and Arneodo, A. Wavelets based estimators of scaling behavior. *IEEE, Trans. in Information Theory.* 2002; **48**, 2938-2954.

[5] Beran, J. *Statistics for Long Memory Processes*, New York: Champan & Hall, 1994.

[6] Celani, A, and Vergassola, M. Statistical geometry in scalar turbulence. *Phys. Rev. Lett.* 2001; **86**, 424-427.

[7] Coeurjolly, JF. Simulation and identification of the fractional Brownian motion: a bibliographical and comparative study. *Journal of statistical software*. 2000; **07**.

[8] Ellis, R. Large deviations for a general class of random vectors. *Ann. Prob.* 1984; **12**:1-12.

[9] Frisch, U and Parisi, G. Fully developed turbulence and intermittency. *Proceeding of Intenational School in Physics*, 1985

[10] Ghashghaie, S, Breymann, W, Peinke, J, Talkner, P and Dodge Y.Turbulent cascades in foreign exchange markets, *Nature.* 1996; **381**, 767-770.

[11] Gonçalvès, P, Riedi, RH and Baraniuk, RG. Simple Statistical Analysis of Wavelet-based Multifractal Spectrum Estimation. *Proceedings of the 32nd Conference on 'Signals, Systems and Computers'*, Asilomar, Nov 1998

[12] Hastie, T, Tibshirani, R and Friedman, J *The Elements of Statistical Learning: Data Mining, Inference, and Prediction.* Springer, 1999.

[13] Hurst, HE. Long-Term Storage Capacity of Reservoirs. *Proc. American Society of Civil Engineering.* 1950; **76**.

[14] Jaffard, S. Local behavior of Riemanns function, *Contemporary Mathematics.* 1995; **189**.

[15] Katul, G, Hsieh, I and Sigmon, J. Energy-inertial scale interaction for temperature and velocity in the unstable surface layer. *Boundary Layer Meteorology.* 1997; **82**:, 49-80.

[16] Katul, G, Vidakovic, B and Albertson, J. Estimating global and local scaling exponents in turbulent flows using wavelet transformations. *Physics of Fluids.* 2000; **13**, 241-250.

[17] Madndelbrot, B et al. Fractional Brownian Motion, Fractional Noise and Applications, *SIAM review.* 1968; **10**, 422-437.

[18] Mandelbrot, B, Calvet, L, Fisher, A. A Multifractal Model of Asset Returns. *Yale University Cowles Foundation Discussion Paper*, **#1164**, 1997.

[19] Mantegna, RN, Stanley, HE.Turbulence and financial markets, *Nature.* 1996; **383**, 587-589.

[20] Prasad, RR, Meneveau, C and Sreenivasan,KR. Multifractal nature of the dissipation field of passive scalars in fully turbulent flows *Physical Review Letters.* 1988; *61*, 74-77.

[21] Riedi, R. *Multifractal Processes, Long range dependence: Theory and Applications.* Eds. Doukhan, Oppenheim and Taqqu, (In-Press),2002.

[22] Riedi, R. Multifractal processes.*Stoch. Proc. Appl., preprint http://citeseer.nj.nec.com/riedi99multifractal.html*, 1999.

[23] Shi, B, Vidakovic, B, Katul, G and Albertson, J. Assessing the Effects of Atmospheric Stability on Inertial Subrange Turbulence using Multiscale Approaches. *Technical report , ISyE, Georgia Tech*, 2003.

[24] Vehel, J, Lutton, E and Tricotn, C. *Fractals in engineering from theory to industrial applications*, Springer Verlag, 1997.

[25] Warhaft, Z, Passive scalars in turbulent flows, *Annual Reviews of Fluid Mechanics.* 2000; **32**, 203-240.